Available online at www.sciencedirect.com
ScienceDirect
Journal of Sound and Vibration 313 (2008) 841–857
JOURNAL OF SOUND AND VIBRATION
www.elsevier.com/locate/jsvi

Effect of non-proportional damping on the torque roll axis decoupling of an engine mounting system

Jae-Yeol Park, Rajendra Singh*

Acoustics and Dynamics Laboratory, Mechanical Engineering Department, Smart Vehicle Concepts Center, The Ohio State University, Columbus, OH 43210, USA

Received 21 August 2007; received in revised form 16 November 2007; accepted 3 December 2007
Available online 9 January 2008

Abstract

Several mounting system design concepts are conceptually used to decouple the engine roll mode though limited success has been observed in practice. One shortcoming of the existing theories or design methods is that they ignore non-proportional viscous damping in their formulations. It seems that the rigid-body vibrations are coupled whenever non-proportional damping is introduced to the mounting system even though the torque roll axis decoupling is still theoretically possible with proportional damping assumption. To overcome this deficiency, we re-formulate the problem for a non-proportionally damped linear system while recognizing that significant damping may be possible with passive (such as hydraulic) or adaptive mounts. The complex mode method is employed in our work and the torque roll axis decoupling paradigm is re-examined given mount rate ratios, mount locations and orientation angles as key design parameters. We derive a necessary axiom for a mode in the torque roll axis direction provided two eigenvalue problems, in terms of stiffness and damping matrices, are concurrently satisfied. Two numerical examples are chosen to examine both steady-state and transient responses and the extent of coupling or decoupling is quantified. Results show that the torque roll axis for a mounting system with non-proportional damping (under oscillating torque excitation) is indeed decoupled when one of the damped modes lies in the torque roll axis direction. Finally, eigensolutions are validated by using experimental data.

1. Introduction

Decoupling of the torque roll axis (TRA) in engine mounting systems has gained much interest given recent developments in the engine deactivation strategies that tend to enhance the dynamic torques. Jeong and Singh [1] have surveyed the prior literature and discussed various mounting system design methods and they had also proposed the TRA decoupling concept using analytical axioms. Unlike other decoupling methods such as the focalization method [2], their method yields complete decoupling between roll and other motions (bounce, yaw, pitch, etc.). Bang et al. [3] conceptually applied the TRA decoupling mounting scheme to experimentally and computationally study the transient vehicle vibration during the key on/off operation. Even though there

*Corresponding author. Tel.: +1 614 292 9044; fax: +1 614 292 3163.
E-mail address: singh.3@osu.edu (R. Singh).

0022-460X/$ - see front matter © 2007 Elsevier Ltd. All rights reserved.
doi:10.1016/j.jsv.2007.12.007

is significant vehicle vibration due to coupling between roll and fore-and-aft modes, they found improvements by partially decoupling the powertrain roll mode from other modes under transient torques. Jeong and Singh [1] and Bang et al. [3] have, however, assumed a proportionally damped system though in reality the viscous damping matrix **C** is often non-proportional given highly damped mounts at one or more locations. For instance, consider the practical case when one or two hydraulic (or adaptive) mounts are utilized along with rubber mounts; the resulting mount parameters are often frequency-dependent and amplitude-sensitive. Nevertheless, the linearized mounting system formulation will yield a non-proportional damping matrix $\mathbf{C}_N$. In fact, Yu et al. [4] have concluded (in their review paper) that further work is needed to examine the range of stiffness and damping properties seen with different mounts and mounting systems. In this paper, we extend the work of Jeong and Singh [1] and comparatively evaluate undamped, proportionally damped, and non-proportionally damped six-degree-of-freedom (6-dof) powertrain mounting systems. The extent of TRA decoupling will be quantified first in terms of the eigensolutions and frequency-response functions given harmonic torque about the crankshaft axis. Transient responses to an impulse torque will also be examined.

2. Problem formulation and TRA decoupling

2.1. Problem statement

Fig. 1 illustrates a typical powertrain isolation system composed of an inertial body, a rigid chassis (foundation), and three or four mounts that could be placed at any exterior point and oriented at any angle. The powertrain is assumed to be a rigid body of dimension six with time-invariant inertial property. Each engine mount is described by three tri-axial spring elements and their stiffness values are assumed to be constant and insensitive to the excitation amplitude. Each mount element is associated with viscous (or structural) damping characteristics. As a result of the assumptions made above, our model is limited to the lower frequency range. Over middle and higher frequency regimes, the powertain body and chassis are expected to be compliant and the mount itself could even exhibit the standing wave effect [5]; the flexibility of foundation (chassis) should be incorporated when the excitation is close to the natural frequencies of compliant base [6,7]. Though any excitation forces can be applied to the rigid powertrain, we will only consider the torque excitation in this paper. Since the analytical models for a mounting system are well established [1,2,6–9], we summarize the basic formulation and then add the general viscous damping **C**. The

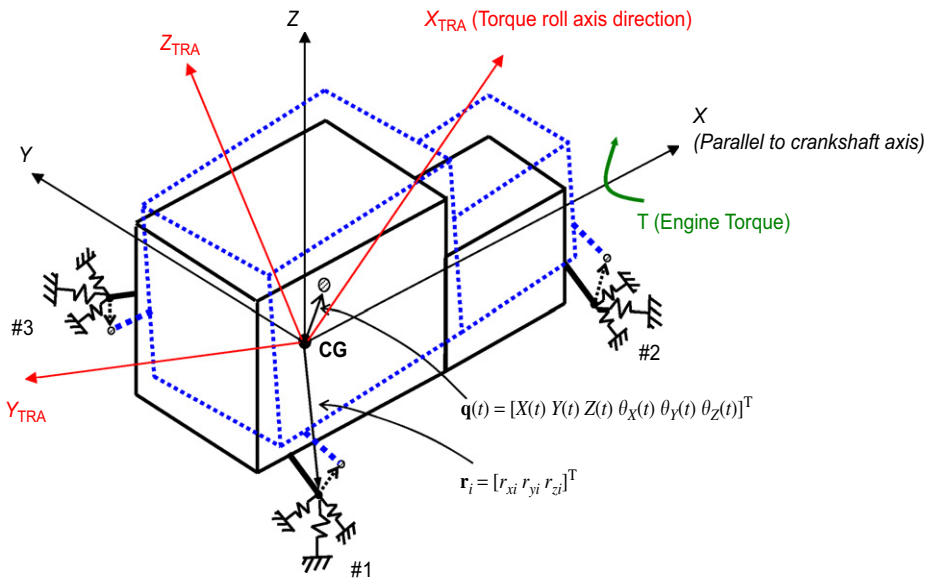

Fig. 1. Typical powertrain isolation system with inclined tri-axial stiffness elements. Both $(XYZ)_g$ and $(XYZ)_{TRA}$ are depicted but mount damping elements are not shown.

following three coordinate systems are used in our work: Inertial coordinates $(XYZ)_g$, TRA coordinates $(XYZ)_{\mathrm{TRA}}$, and local mount coordinates $(XYZ)_{mi}$, $i = 1, \ldots, n$ where n is the number of mounts. The $(XYZ)_g$ coordinate system is a ground-fixed reference frame with its origin at the static equilibrium (at the centre of gravity (CG)). The displacements of supported inertial body are assumed to be small and the displacement vector $\mathbf{q}(t) = [XYZ\ \theta_x\ \theta_y\ \theta_z]^{\mathrm{T}}(t)$ can be completely expressed by the translational and angular displacements of the CG. The governing equations of motion are formulated in matrix form, as shown below, where $\dot{\mathbf{q}}(t)$ and $\ddot{\mathbf{q}}(t)$ are the velocity, and acceleration vectors, respectively, of dimension six:

$$\mathbf{M}\ddot{\mathbf{q}}(t) + \mathbf{C}\dot{\mathbf{q}}(t) + \mathbf{K}\mathbf{q}(t) = \mathbf{f}(t). \tag{1}$$

Here, $\mathbf{M}$ is the inertial (mass) matrix, $\mathbf{K}$ the stiffness matrix, $\mathbf{C}$ the viscous damping matrix (assuming non-proportional damping), and $\mathbf{f}(t)$ the external excitation (force/torque) vector. The localized stiffness and damping matrices, $\mathbf{K}_{mi}$ and $\mathbf{C}_{mi}$, in the local $(XYZ)_{mi}$ coordinate systems at each mount are expressed as follows:

$$\mathbf{K}_{mi} = \begin{bmatrix} k_{ai} & 0 & 0 \\ & k_{bi} & 0 \\ \text{sym.} & & k_{ci} \end{bmatrix}, \quad \mathbf{C}_{mi} = \begin{bmatrix} c_{ai} & 0 & 0 \\ & c_{bi} & 0 \\ \text{sym.} & & c_{ci} \end{bmatrix}. \tag{2a,b}$$

Here, k_a is the principal compressive stiffness, and k_b and k_c are the principal shear stiffness components. Likewise, define c_a as the principal compressive damping, and c_b and c_c as the principal shear damping coefficients. Both matrices are transformed and expressed with respect to the global $(XYZ)_g$ coordinate system using a rotational matrix, $\mathbf{\Theta}_{g,mi}$, derived from the orientation angles of each mount:

$$\mathbf{K}_{g,mi} = \mathbf{\Theta}_{g,mi}\mathbf{K}_{mi}\mathbf{\Theta}_{g,mi}^{\mathrm{T}} = \begin{bmatrix} k_{xxi} & k_{xyi} & k_{xzi} \\ & k_{yyi} & k_{yzi} \\ \text{sym.} & & k_{zzi} \end{bmatrix}, \tag{3a}$$

$$\mathbf{C}_{g,mi} = \mathbf{\Theta}_{g,mi}\mathbf{C}_{mi}\mathbf{\Theta}_{g,mi}^{\mathrm{T}} = \begin{bmatrix} c_{xxi} & c_{xyi} & c_{xzi} \\ & c_{yyi} & c_{yzi} \\ \text{sym.} & & c_{zzi} \end{bmatrix}. \tag{3b}$$

Using the Euler angles as given by $(\theta_i, \varphi_i, \phi_i)$ for ith mount, the rotational matrix, $\mathbf{\Theta}_{g,mi}$ is found by rotating about axes of $(XYZ)_g$ in the order of X, Y, and Z. It includes a product of three rotational matrix operators as shown below:

$$\mathbf{\Theta}_{g,mi} = \begin{bmatrix} \cos\varphi_i \cos\phi_i & \cos\theta_i \sin\phi_i + \sin\theta_i \sin\varphi_i \cos\phi_i & \sin\theta_i \sin\phi_i - \cos\theta_i \sin\varphi_i \cos\phi_i \\ -\cos\varphi_i \sin\phi_i & \cos\theta_i \cos\phi_i - \sin\theta_i \sin\varphi_i \sin\phi_i & \sin\theta_i \cos\phi_i + \cos\theta_i \sin\varphi_i \sin\phi_i \\ \sin\varphi_i & -\sin\theta_i \cos\varphi_i & \cos\theta_i \cos\varphi_i \end{bmatrix}. \tag{4}$$

Since the displacements at the mount location(s) caused by the rigid-body rotations are computed by using a cross-vector product, the resulting deflection, $\mathbf{q}_{mi,t}(t)$, at each mount is as follows based on the rigid foundation assumption:

$$\mathbf{q}_{mi,t}(t) = \mathbf{q}_t(t) + \mathbf{q}_\theta(t) \times \mathbf{r}_{mi} \tag{5}$$

in which $\mathbf{r}_{mi} = [r_{xi}\ r_{yi}\ r_{zi}]^{\mathrm{T}}$ is the position vector of each mount and $\mathbf{q}_t(t) = [XYZ]^{\mathrm{T}}(t)$ and $\mathbf{q}_\theta(t) = [\theta_X\ \theta_Y\ \theta_Z]^{\mathrm{T}}(t)$ are the translational and rotational displacements of powertrain. The cross-vector in Eq. (5) can be expressed by a tensor skew matrix, $\mathbf{L}_{mi}$:

$$\mathbf{q}_{mi,t}(t) = [\,\mathbf{I} \quad \mathbf{L}_{mi}\,]\mathbf{q}(t), \tag{6}$$

$$\mathbf{L}_{mi} = \begin{bmatrix} 0 & r_{zi} & -r_{yi} \\ & 0 & r_{xi} \\ \text{skew sym.} & & 0 \end{bmatrix}. \tag{7}$$

Translational and rotational reaction force $\mathbf{f}_{mi,t}(t)$ and moment $\mathbf{f}_{mi,\theta}(t)$ due to the vibratory displacement and velocity at each mount are calculated as follows:

$$\begin{aligned}\mathbf{f}_{mi,t}(t) &= -\mathbf{K}_{g,mi}\mathbf{q}_{mi,t}(t) - \mathbf{C}_{g,mi}\dot{\mathbf{q}}_{mi,t}(t)\\ &= -\begin{bmatrix}\mathbf{K}_{g,mi} & \mathbf{K}_{g,mi}\mathbf{L}_{mi}\end{bmatrix}\mathbf{q}(t) - \begin{bmatrix}\mathbf{C}_{g,mi} & \mathbf{C}_{g,mi}\mathbf{L}_{mi}\end{bmatrix}\dot{\mathbf{q}}(t),\end{aligned} \tag{8}$$

$$\begin{aligned}\mathbf{f}_{mi,\theta}(t) &= \mathbf{r}_{mi}\times\mathbf{f}_{mi,t}(t) = \mathbf{L}_{mi}^{\mathrm{T}}\mathbf{f}_{mi,t}(t)\\ &= -\begin{bmatrix}\mathbf{L}_{mi}^{\mathrm{T}}\mathbf{K}_{g,mi} & \mathbf{L}_{mi}^{\mathrm{T}}\mathbf{K}_{g,mi}\mathbf{L}_{mi}\end{bmatrix}\mathbf{q}(t) - \begin{bmatrix}\mathbf{L}_{mi}^{\mathrm{T}}\mathbf{C}_{g,mi} & \mathbf{L}_{mi}^{\mathrm{T}}\mathbf{C}_{g,mi}\mathbf{L}_{mi}\end{bmatrix}\dot{\mathbf{q}}(t).\end{aligned} \tag{9}$$

Combining Eqs. (8) and (9), we construct the global stiffness $\mathbf{K}$ and damping $\mathbf{C}$ matrices with respect to the inertial coordinate system for the powertrain mounting system with n number of mounts:

$$\mathbf{K} = \sum_{i=1}^{n}\mathbf{K}_i = \sum_{i=1}^{n}\begin{bmatrix}\mathbf{K}_{g,mi} & \mathbf{K}_{g,mi}\mathbf{L}_{mi}\\ \mathbf{L}_{mi}^{\mathrm{T}}\mathbf{K}_{g,mi} & \mathbf{L}_{mi}^{\mathrm{T}}\mathbf{K}_{g,mi}\mathbf{L}_{mi}\end{bmatrix}, \tag{10a}$$

$$\mathbf{C} = \sum_{i=1}^{n}\mathbf{C}_i = \sum_{i=1}^{n}\begin{bmatrix}\mathbf{C}_{g,mi} & \mathbf{C}_{g,mi}\mathbf{L}_{mi}\\ \mathbf{L}_{mi}^{\mathrm{T}}\mathbf{C}_{g,mi} & \mathbf{L}_{mi}^{\mathrm{T}}\mathbf{C}_{g,mi}\mathbf{L}_{mi}\end{bmatrix}. \tag{10b}$$

Eventually, we can assemble the governing equations as given by Eq. (1). Even though the general damping matrix ($\mathbf{C}$) (such as in Eq. (10b)) is typically formulated before, it is still not considered in any dynamic analysis [1,4,6–9]; undamped or proportional damping assumption has been invariably employed. It is quite clear from the formulation that $\mathbf{C}$ will not allow a decoupling of the equations in the modal domain. Accordingly, specific objectives of this article are as follows: (1) examine the effect of non-proportional damping on the TRA decoupling axioms [1]; (2) propose new analytical conditions that will still yield an uncoupled system in the presence of non-proportional damping; (3) provide illustrative examples in frequency and time domains, as well as comparison of eigensolutions with experimental data.

2.2. TRA decoupling with proportional damping

A TRA is uniquely defined by both inertial properties and applied torque direction for an unconstrained rigid body with small motions given only one-dimensional dynamic torque [1]. The resulting modes from the eigenvalue problem for a proportionally damped system will yield the same eigenvectors as those of the corresponding undamped problem. Using this property and letting one of the modes be in the TRA direction, we can prove that the TRA decoupling for a proportionally damped system is achieved as follows. Apply the harmonic torque excitation as $\mathbf{f}(t) = \mathbf{T}\mathrm{e}^{\mathrm{j}\omega t}$ in Eq. (1) and then assume the steady-state harmonic response is in the form of $\mathbf{q}(t) = \mathbf{Q}\mathrm{e}^{\mathrm{j}\omega t}$ we obtain

$$-\omega^2\mathbf{M}\mathbf{Q} + \mathrm{j}\omega\mathbf{C}_P\mathbf{Q} + \mathbf{K}\mathbf{Q} = \mathbf{T} \tag{11}$$

in which $\mathbf{C}_p$ is proportional damping matrix. The dynamic response of the 6-dof system is expressed by $\mathbf{Q} = \sum_{r=1}^{N} b_r\mathbf{u}_r$, where, $\mathbf{u}_r$ are eigenvectors, b_r are the modal participation coefficients and N is the number of modes. Next, we employ the orthogonal property ($\mathbf{u}_r^{\mathrm{T}}\mathbf{M}\mathbf{u}_s = \delta_{rs}$, $\mathbf{u}_r^{\mathrm{T}}\mathbf{K}\mathbf{u}_s = k_r\delta_{rs}$, $r,s = 1,2,\ldots,N$ where δ_{rs} is the Kroneker delta function) to get

$$-\omega^2 b_r + \mathrm{j}\omega\mathbf{u}_r^{\mathrm{T}}\mathbf{C}_P\sum_{s=1}^{N} b_s\mathbf{u}_s + b_r k_r = \mathbf{u}_r^{\mathrm{T}}\mathbf{T}. \tag{12}$$

If we were to assume the Rayleigh damping model ($\mathbf{C}_p = \alpha\mathbf{M} + \beta\mathbf{K}$, where α and β are arbitrary scalar values), we could write Eq. (12) as

$$b_r = \frac{\mathbf{u}_r^{\mathrm{T}}\mathbf{T}}{-\omega^2 + \mathrm{j}\omega(\alpha + \beta k_r) + k_r}. \tag{13}$$

On the other hand, one of the modes is selected to be parallel to the TRA direction and it is defined as $\mathbf{q}_{\mathrm{TRA}}$. Let one mode, $\mathbf{u}_s$, be in the TRA direction as follows and use scalar constants, γ and ρ to yield the following:

$$\mathbf{q}_{\mathrm{TRA}} = \gamma \mathbf{M}^{-1}\mathbf{T} \quad \text{and} \quad \mathbf{u}_s = \rho \mathbf{q}_{\mathrm{TRA}}. \tag{14a,b}$$

Combining Eqs. (14a,b), we obtain

$$\mathbf{u}_r^{\mathrm{T}}\mathbf{T} = \frac{\mathbf{u}_r^{\mathrm{T}}\mathbf{M}\mathbf{u}_s}{\gamma\rho} = \frac{1}{\gamma\rho}\delta_{rs}, \quad r,s = 1,2,\ldots,N. \tag{15}$$

From Eqs. (13) and (15), only $b_s \neq 0$ and $b_r = 0$. Eventually, the resulting motion, $\mathbf{q}(t)$, exists only in the TRA direction for a proportionally damped dynamic system. This is consistent with the axiom proposed by Jeong and Singh [1]. Next consider Eq. (1) with $\mathbf{f}(t) = \mathbf{0}$ leading to $\mathbf{M}\ddot{\mathbf{q}}(t) + \mathbf{C}\dot{\mathbf{q}}(t) + \mathbf{K}\mathbf{q}(t) = \mathbf{0}$. Assume the solution as $\mathbf{q}(t) = \mathrm{e}^{\lambda t}\mathbf{u}$ where λ is a scalar constant and $\mathbf{u}$ is a constant vector, though both could be complex valued. Accordingly, we get $\lambda^2\mathbf{M}\mathbf{u} + \lambda\mathbf{C}\mathbf{u} + \mathbf{K}\mathbf{u} = \mathbf{0}$. Assuming that $\lambda = \tau + \mathrm{j}\eta$ and letting one of the modes be in the TRA direction ($\mathbf{u} = \mathbf{q}_{\mathrm{TRA}}$) we obtain the following eigenvalue problem:

$$(\tau + \mathrm{j}\eta)^2\mathbf{M}\mathbf{q}_{\mathrm{TRA}} + (\tau + \mathrm{j}\eta)\mathbf{C}\mathbf{q}_{\mathrm{TRA}} + \mathbf{K}\mathbf{q}_{\mathrm{TRA}} = \mathbf{0}. \tag{16}$$

For the proportional damping case ($\mathbf{C} = \mathbf{C}_p$), grouping the above equation in terms of real and imaginary parts, we have

$$[(\tau^2 - \eta^2 + \tau\alpha)\mathbf{M} + (1 + \tau\beta)\mathbf{K}]\mathbf{q}_{\mathrm{TRA}} + \mathrm{j}[(2\tau\eta + \eta\alpha)\mathbf{M} + \eta\beta\mathbf{K}]\mathbf{q}_{\mathrm{TRA}} = \mathbf{0}. \tag{17}$$

Solving Eq. (17) and considering the fact that $\mathbf{M}\mathbf{q}_{\mathrm{TRA}} \| \mathbf{T}$, we find that the corresponding eigenvalue problem for a proportionally damped mounting is given by $\mathbf{K}\mathbf{q}_{\mathrm{TRA}} = \lambda_k\mathbf{M}\mathbf{q}_{\mathrm{TRA}}$. This condition was shown previously, for an undamped system, by Jeong and Singh [1].

3. Effect of non-proportional damping on the TRA decoupling

3.1. Example case

The effect of non-proportional damping on motion coupling is examined for one example—a V6 diesel engine [8] whose mounting system parameters (stiffness values, mount locations, and orientation angles) are given in Table 1. Real and complex eigensolutions for the nominal values of mount parameters are calculated and compared with measured natural frequencies in Table 2. Our analysis suggests that the measured natural frequency at 12.47 Hz corresponds to the sixth (and not the fifth) mode. Perturbations are applied about the nominal values of engine inertial data and mount orientation angles and the corresponding eigensolutions are

Table 1
Mount parameters values for the V6 diesel engine example

Mount parameters	Mount #			
	1	2	3	4
Stiffness ($\mathrm{N\,mm^{-1}}$)				
k_a	224	170	217	232
k_b	45	126	434	464
k_c	45	49	109	116
Location (mm)				
r_x	−225	361	−195	293
r_y	−309	−282	141	167
r_z	−199	−251	229	−245
Orientation (deg)				
θ	0	0	0	0
φ	−45	−39	−75	−45
ϕ	0	180	0	180

Table 2
Comparison of calculated and measured natural frequencies

Mode	Natural frequencies (Hz)				
	Measured	Undamped (real eigensolution)		Damped (complex eigensolution)	
		With nominal parameters	Perturbed[a] about the nominal values	With nominal parameters	Perturbed about the nominal values
1	4.17	4.47	4.31	4.43 ($\zeta^{b}=16\%$)	4.34 ($\zeta=16\%$)
2	5.66	5.97	5.86	5.83 ($\zeta=23\%$)	5.75 ($\zeta=23\%$)
3	6.47	7.48	7.40	7.13 ($\zeta=30\%$)	7.05 ($\zeta=29\%$)
4	8.76	9.87	9.65	9.00 ($\zeta=41\%$)	8.91 ($\zeta=41\%$)
5	–	12.27	12.42	10.79 ($\zeta=47\%$)	10.86 ($\zeta=49\%$)
6	12.47	16.45	16.48	12.49 ($\zeta=65\%$)	12.56 ($\zeta=64\%$)

[a]Perturbation is applied about the nominal inertial parameters (up to 5%) and orientation angles (up to 12%).
[b]ζ is the modal damping ratio.

also computed as reported in Table 2. We achieve a better agreement with measured data when the complex eigensolution method with non-proportional damping is used and mounting parameters are perturbed about the nominal values. This implies that the real V6 engine mounting system is indeed non-proportionally damped. Frequency-response functions for the TRA decoupled V6 engine mounting system given harmonic excitation in the crank axis direction are calculated first for the proportional damping as shown in Fig. 2 and then for the non-proportional damping in Fig. 3. Corresponding mounting parameters for the TRA decoupling with proportional damping are given in Table 5. Spectra for the original mounting system (without the TRA decoupled design) are also presented for the sake of comparison. Next, an impulse torque is applied in the crankshaft axis direction and the resulting transient responses are shown in Figs. 4 and 5, respectively, for both damping cases. Observe that a complete decoupling of the motions (that are originally coupled to begin with) is achieved by selecting appropriate mount parameters (stiffness, location, and orientation of mounts) provided that proportional damping exists. In this case, motion exists only in the roll direction θ_X as shown in Fig. 4. But, vibrations are coupled again in Fig. 5 with an introduction of non-proportional damping. Modal analyses are conducted next by using the complex eigensolution method and results are reported in Table 3 for two modes of interest. Coupled eigenvectors corresponding to the roll and vertical bounce modes are found for the non-proportional damping case; conversely, uncoupled eigenvectors exist for the proportional damping case. Two resonant peaks in the z-direction (vertical bounce) spectra are also found in Fig. 3c: both peaks show modal coupling.

3.2. Necessary condition for TRA decoupling

The non-proportionally damped system exhibits complex modes (with arbitrary phase angles) that could differ from the real modes (with 0° or 180° phase) for proportionally damped system. Governing equations for mounting system (with $\mathbf{C}_N$ as non-proportional damping matrix) in the inertial coordinate system are expressed in state-space form (2 N space) as follows:

$$\mathbf{A}\dot{\mathbf{p}}(t)+\mathbf{B}\mathbf{p}(t)=\mathbf{g}(t), \tag{18}$$

$$\mathbf{A}=\begin{bmatrix}\mathbf{M} & \mathbf{0}\\ \mathbf{0} & -\mathbf{K}\end{bmatrix},\quad \mathbf{B}=\begin{bmatrix}\mathbf{C}_N & \mathbf{K}\\ \mathbf{K} & \mathbf{0}\end{bmatrix},\quad \mathbf{p}(t)=\begin{bmatrix}\dot{\mathbf{q}}(t)\\ \mathbf{q}(t)\end{bmatrix},\quad \mathbf{g}(t)=\begin{bmatrix}\mathbf{f}(t)\\ \mathbf{0}\end{bmatrix}. \tag{19a,b,c,d}$$

The resulting eigenvectors are orthogonal with respect to $\mathbf{A}$ and $\mathbf{B}$. Using this property, we can analytically prove that the TRA decoupling for a non-proportionally damped case could still be achieved as follows. Apply the harmonic torque excitation as $\mathbf{f}(t)=\mathbf{T}e^{j\omega t}$ and then the steady-state response will be in the form of

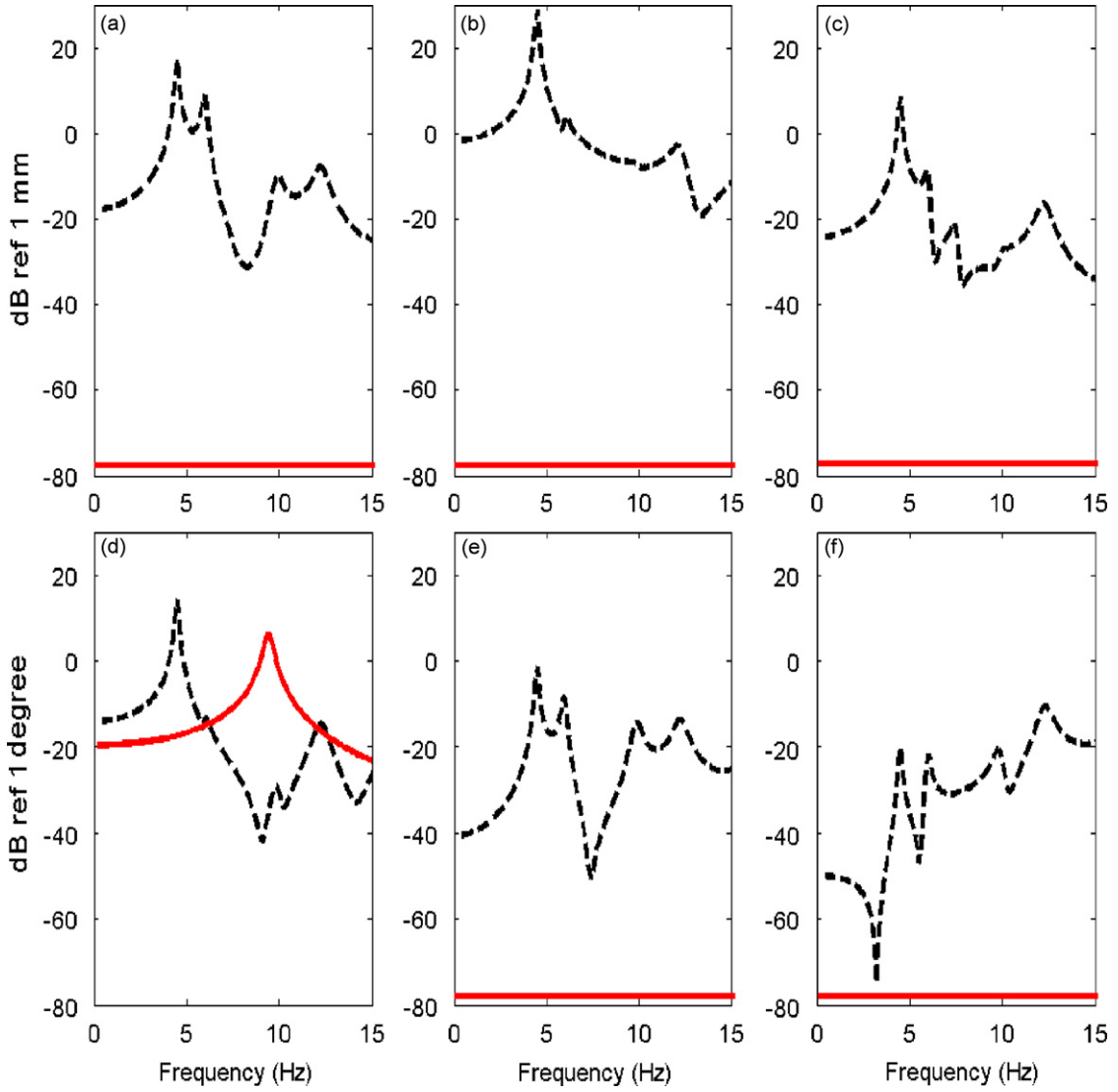

Fig. 2. Frequency-response functions with proportional damping given harmonic torque: (a) $X(\omega)$; (b) $Y(\omega)$; (c) $Z(\omega)$; (d) $\theta_X(\omega)$; (e) $\theta_Y(\omega)$; and (f) $\theta_Z(\omega)$. Key: ▬ ▬, original mounting system; ▬, torque roll axis decoupled mounting system with proportional damping.

$\mathbf{q}(t) = \mathbf{Q}e^{j\omega t}$, leading to

$$j\omega\mathbf{AP} + \mathbf{BP} = \mathbf{G}, \tag{20}$$

$$\mathbf{G} = \begin{bmatrix} \mathbf{T} \\ \mathbf{0} \end{bmatrix}, \quad \mathbf{P} = \begin{bmatrix} j\omega\mathbf{Q} \\ \mathbf{Q} \end{bmatrix}. \tag{21a,b}$$

Based on the orthogonal property of eigenvectors, the dynamic response of the 6-dof system is expressed by $\mathbf{P} = \sum_{r=1}^{2N} b_r \mathbf{U}_r$ where, $\mathbf{U}_r$ are the eigenvectors and b_r are the modal participation coefficients. Orthogonal property of the complex eigenvectors provides the following relations: $\mathbf{U}_r^{\mathrm{T}}\mathbf{A}\mathbf{U}_s = \delta_{rs}$, $\mathbf{U}_r^{\mathrm{T}}\mathbf{B}\mathbf{U}_s = k_r\delta_{rs}$, r, $s = 1,2,\ldots,2N$. Using the orthogonal property, Eq. (20) yields

$$b_r = \frac{\mathbf{U}_r^{\mathrm{T}}\mathbf{G}}{j\omega + k_r}. \tag{22}$$

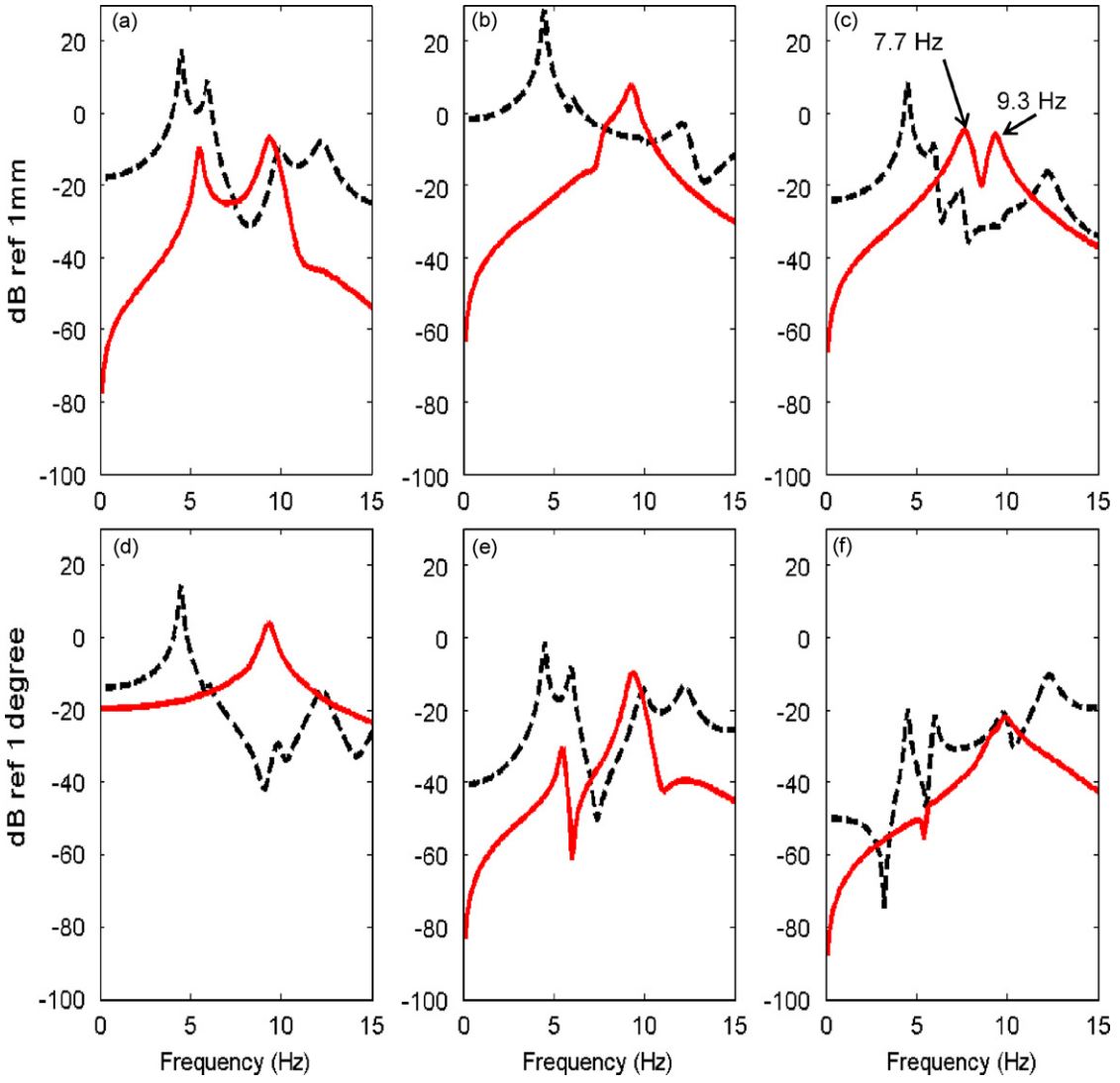

Fig. 3. Frequency-response functions with non-proportional damping given harmonic torque: (a) $X(\omega)$; (b) $Y(\omega)$; (c) $Z(\omega)$; (d) $\theta_X(\omega)$; (e) $\theta_Y(\omega)$; and (f) $\theta_Z(\omega)$. Key: ▬ ▬, original mounting system; ▬, torque roll axis mounting system with non-proportional damping.

In order to achieve the roll mode motion decoupling, on the other hand, it is assumed that one of the eigenvectors should be parallel to the TRA direction. Define the TRA direction, $\mathbf{q}_{\mathrm{TRA}}$, and let one mode, $\mathbf{u}_s$, be in the TRA direction as follows. Here γ and ρ are constants:

$$\mathbf{q}_{\mathrm{TRA}} = \gamma \mathbf{M}^{-1}\mathbf{T}, \tag{23}$$

$$\mathbf{U}_s = \rho \mathbf{P}_{\mathrm{TRA}} \quad \text{where } \mathbf{U}_s = \begin{bmatrix} \lambda \mathbf{u}_s \\ \mathbf{u}_s \end{bmatrix} \quad \text{and} \quad \mathbf{P}_{\mathrm{TRA}} = \begin{bmatrix} \lambda \mathbf{q}_{\mathrm{TRA}} \\ \mathbf{q}_{\mathrm{TRA}} \end{bmatrix}. \tag{24}$$

Combining Eqs. (23) and (24) and using $\mathbf{U}_r^{\mathrm{T}}\mathbf{A}\mathbf{U}_s = \rho \mathbf{U}_r^{\mathrm{T}} \begin{bmatrix} \mathbf{M} & \mathbf{0} \\ \mathbf{0} & -\mathbf{K} \end{bmatrix} \begin{bmatrix} \lambda \mathbf{q}_{\mathrm{TRA}} \\ \mathbf{q}_{\mathrm{TRA}} \end{bmatrix}$, we obtain

$$\mathbf{U}_r^{\mathrm{T}}\mathbf{G} = \frac{1}{\rho\gamma}\frac{1}{\lambda}\left(\mathbf{U}_r^{\mathrm{T}}\mathbf{A}\mathbf{U}_s + \mathbf{U}_r^{\mathrm{T}} \begin{bmatrix} \mathbf{0} \\ \mathbf{K}\mathbf{u}_s \end{bmatrix}\right). \tag{25a}$$

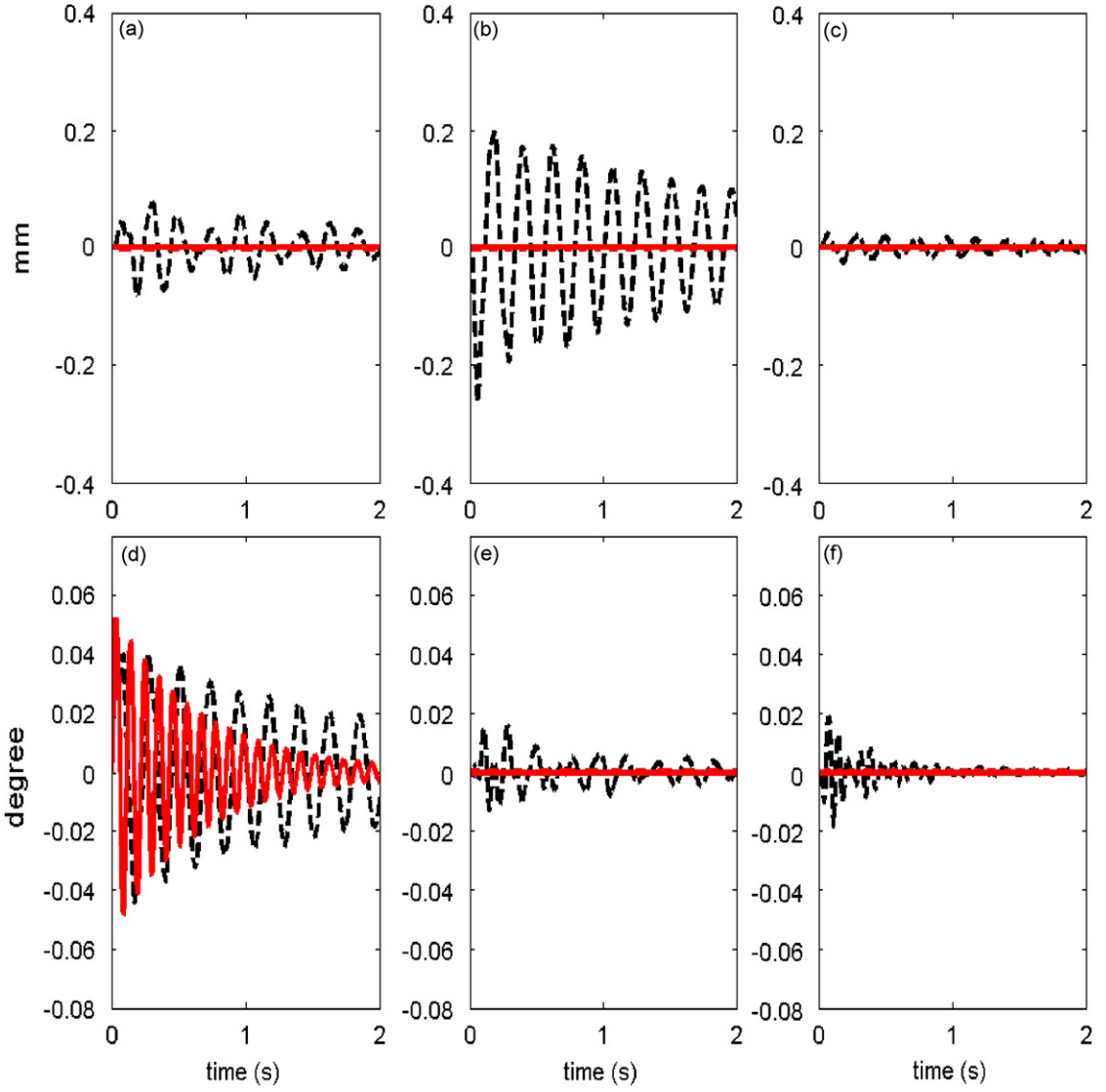

Fig. 4. Impulsive responses with proportional damping given torque impulse: (a) $X(t)$; (b) $Y(t)$; (c) $Z(t)$; (d) $\theta_X(t)$; (e) $\theta_Y(t)$; and (f) $\theta_Z(t)$. Key: ▬ ▬, original; ▬, torque roll axis with proportional damping.

Expand the above to yield

$$\mathbf{U}_r^{\mathrm{T}}\mathbf{G} = \frac{1}{\rho\gamma}\frac{1}{\lambda}(\delta_{rs} + \mathbf{u}_r^{\mathrm{T}}\mathbf{K}\mathbf{u}_s). \tag{25b}$$

Use the orthogonal property, $\mathbf{U}_r^{\mathrm{T}}\mathbf{B}\mathbf{U}_s = k_r\delta_{rs}$, to rewrite the above as

$$\mathbf{U}_r^{\mathrm{T}}\mathbf{G} = \frac{1}{\rho\gamma}\frac{1}{\lambda}\left\{\left(1 + \frac{k_r}{2\lambda}\right)\delta_{rs} - \frac{\lambda}{2}\mathbf{u}_r^{\mathrm{T}}\mathbf{C}_N\mathbf{u}_s\right\}. \tag{25c}$$

Since $\mathbf{u}_s$ is set in the TRA direction, Eqs. (25a–c) become

$$\mathbf{U}_r^{\mathrm{T}}\mathbf{G} = \frac{1}{\rho\gamma}(1 + a_s)\delta_{rs}. \tag{25d}$$

Here $a_s = \mathbf{u}_s^{\mathrm{T}}\mathbf{K}\mathbf{u}_s$. From Eqs. (22) and (25d), only $b_s \neq 0$ and $b_r = 0$. Eventually, the motion response, $\mathbf{q}(t)$, exists only in the TRA direction for a non-proportionally damped dynamic system.

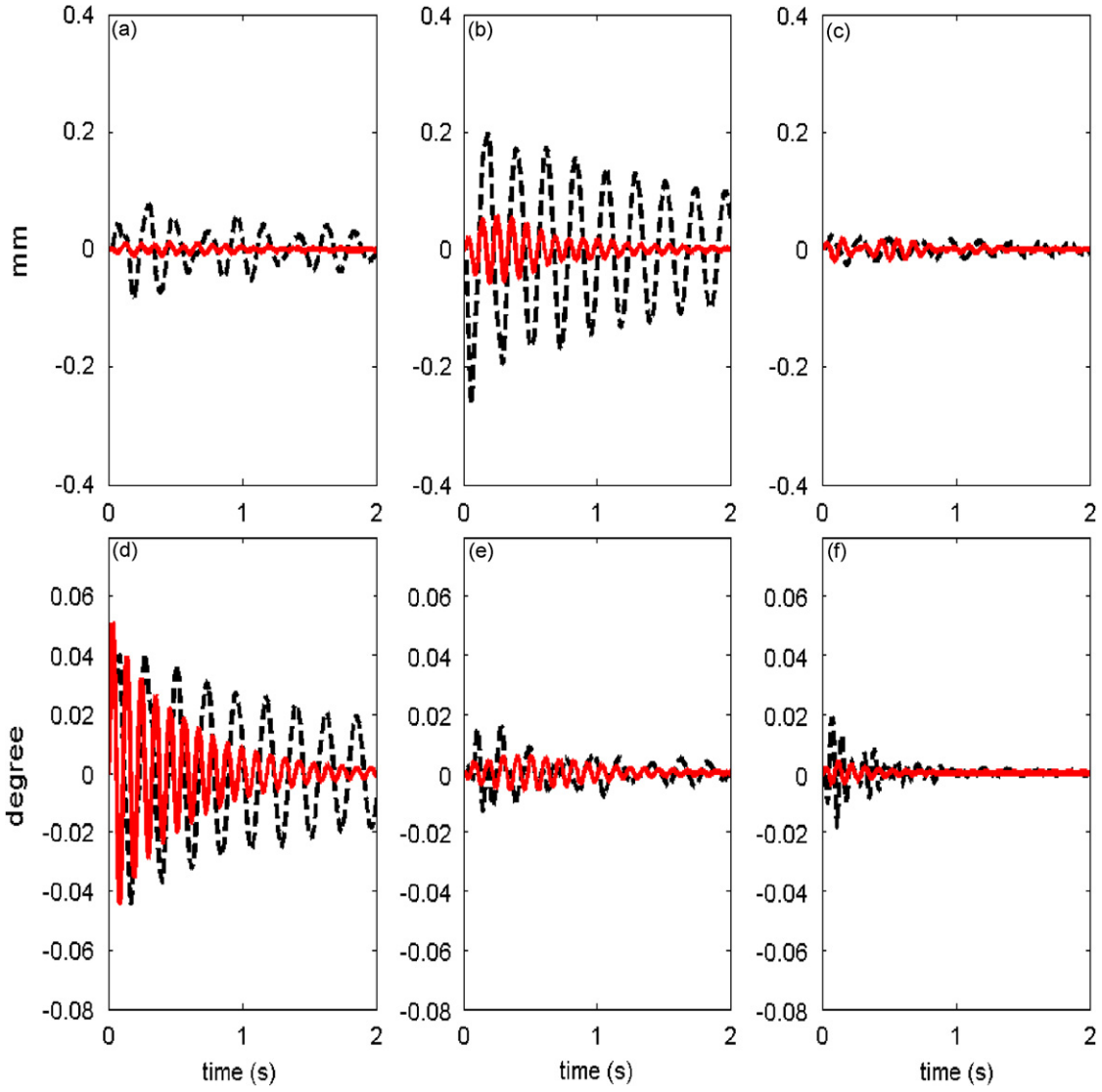

Fig. 5. Impulsive responses with non-proportional damping given torque impulse: (a) $X(t)$; (b) $Y(t)$; (c) $Z(t)$; (d) $\theta_X(t)$; (e) $\theta_Y(t)$; and (f) $\theta_Z(t)$. Key: ▬ ▬, original; ▬, torque roll axis with non-proportional damping.

3.3. Conditions for TRA decoupling with non-proportional damping

In Section 3.2, we assumed that one of the modes is in the TRA direction for non-proportional damping. The corresponding eigenvalue problem, as stated by Eq. (26), must be satisfied:

$$\lambda \mathbf{A}\mathbf{p}_{\mathrm{TRA}} + \mathbf{B}\mathbf{p}_{\mathrm{TRA}} = \mathbf{0}, \tag{26}$$

$$\mathbf{p}_{\mathrm{TRA}} = \begin{bmatrix} \lambda \mathbf{q}_{\mathrm{TRA}} \\ \mathbf{q}_{\mathrm{TRA}} \end{bmatrix}. \tag{27}$$

Eqs. (26) and (27) give us $\lambda^2\mathbf{M}\mathbf{u} + \lambda\mathbf{C}\mathbf{u} + \mathbf{K}\mathbf{u} = \mathbf{0}$, as obtained previously in Section 2.2. For the non-proportional damping case, grouping of the real and imaginary parts from Eq. (16) leads to

$$[(\tau^2 - \eta^2)\mathbf{M} + \tau\mathbf{C}_N + \mathbf{K}]\mathbf{q}_{\mathrm{TRA}} + \mathrm{j}[2\tau\eta\mathbf{M} + \eta\mathbf{C}_N]\mathbf{q}_{\mathrm{TRA}} = \mathbf{0}. \tag{28}$$

Table 3
Roll and bounce eigenvectors (**u**) and damping ratios (ζ) with proportional ($\mathbf{C}_p$) and non-proportional ($\mathbf{C}_N$) damping cases

Dominant mode		Roll θ_x		Vertical X (bounce)	
C		$\mathbf{C}_p$	$\mathbf{C}_N$	$\mathbf{C}_p$	$\mathbf{C}_N$
u	$\lvert X\rvert$	0	0.02	0	0.01
	$\lvert Y\rvert$	0	0.10	0	0.54
	$\lvert Z\rvert$	0	0.02	1	1.00
	$\lvert\theta_X\rvert$	1	1.00	0	0.52
	$\lvert\theta_Y\rvert$	0	0.27	0	0.05
	$\lvert\theta_Z\rvert$	0	0.01	0	0.01
ζ (%)		2.1	3.1	2.5	4.6

Units of eigenvector elements: mm for X, Y, and Z; degree (deg) for θ_X, θ_Y, and θ_Z.

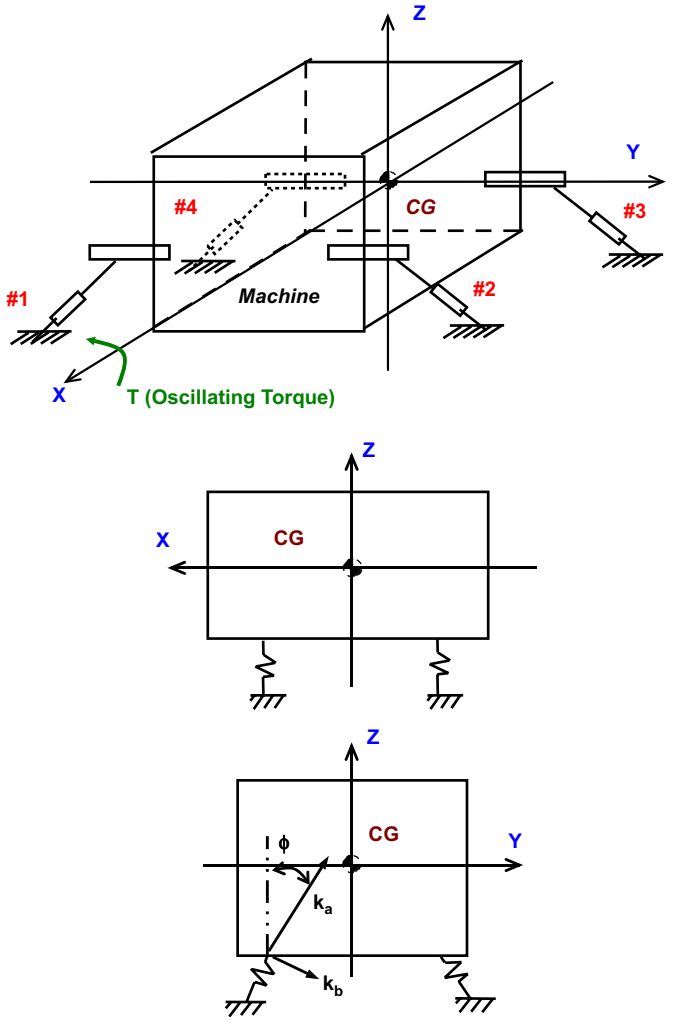

Fig. 6. Focalized mounting system.

In order to satisfy Eq. (28), we must solve two equations in terms of real and imaginary parts, as expressed below, using the fact that $\mathbf{q}_{\mathrm{TRA}}$ is a real-valued eigenvector:

$$[(\tau^2-\eta^2)\mathbf{M}+\tau\mathbf{C}_N+\mathbf{K}]\mathbf{q}_{\mathrm{TRA}}=\mathbf{0} \quad \text{and} \quad [2\tau\eta\mathbf{M}+\eta\mathbf{C}_N]\mathbf{q}_{\mathrm{TRA}}=\mathbf{0}. \tag{29a,b}$$

Solving Eqs. (29a,b) and considering the fact that $\mathbf{M}\mathbf{q}_{\mathrm{TRA}}\|\mathbf{T}$, we obtain $\mathbf{K}\mathbf{q}_{\mathrm{TRA}}\|\mathbf{T}$ and $\mathbf{C}_N\mathbf{q}_{\mathrm{TRA}}\|\mathbf{T}$. Thus, $\mathbf{K}\mathbf{q}_{\mathrm{TRA}}\|\mathbf{M}\mathbf{q}_{\mathrm{TRA}}$ and $\mathbf{C}_N\mathbf{q}_{\mathrm{TRA}}\|\mathbf{M}\mathbf{q}_{\mathrm{TRA}}$. These lead to two concurrent eigenvalue problems:

$$\mathbf{K}\mathbf{q}_{\mathrm{TRA}}=\lambda_k\mathbf{M}\mathbf{q}_{\mathrm{TRA}} \quad \text{and} \quad \mathbf{C}_N\mathbf{q}_{\mathrm{TRA}}=\lambda_c\mathbf{M}\mathbf{q}_{\mathrm{TRA}}. \tag{30a,b}$$

These are different from the conventional eigenvalue problems since the $\mathbf{K}$ and $\mathbf{C}_N$ must be constructed for the mounting system. Further, the eigenvlaue problem for non-proportional damping case is associated with both stiffness and damping matrixes as given by Eqs. (30a,b). For the proportional damping case (with $\mathbf{C}_p=\alpha\mathbf{M}+\beta\mathbf{K}$), the two eigenvalues, λ_k and λ_c are related as $\lambda_c=\alpha+\beta\lambda_k$. Both eigenvalues, $\lambda_k(=\tau^2+\eta^2)$ and

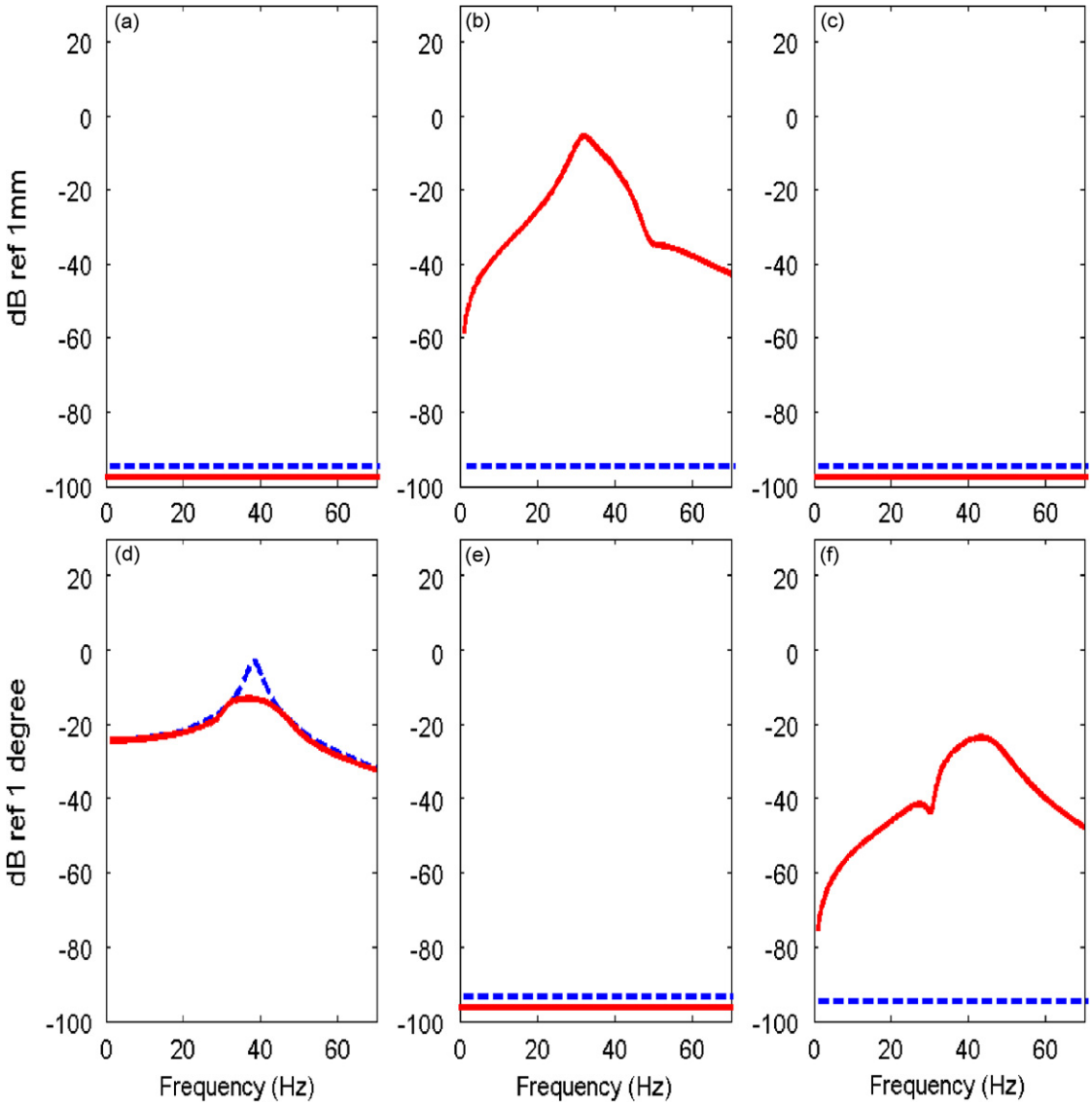

Fig. 7. Frequency-response functions given harmonic torque with torque roll axis decoupling scheme for proportional damping applied: (a) $X(\omega)$; (b) $Y(\omega)$; (c) $Z(\omega)$; (d) $\theta_X(\omega)$; (e) $\theta_Y(\omega)$; and (f) $\theta_Z(\omega)$. Key: — —, mounting system with proportional damping; ——, mounting system with non-proportional damping.

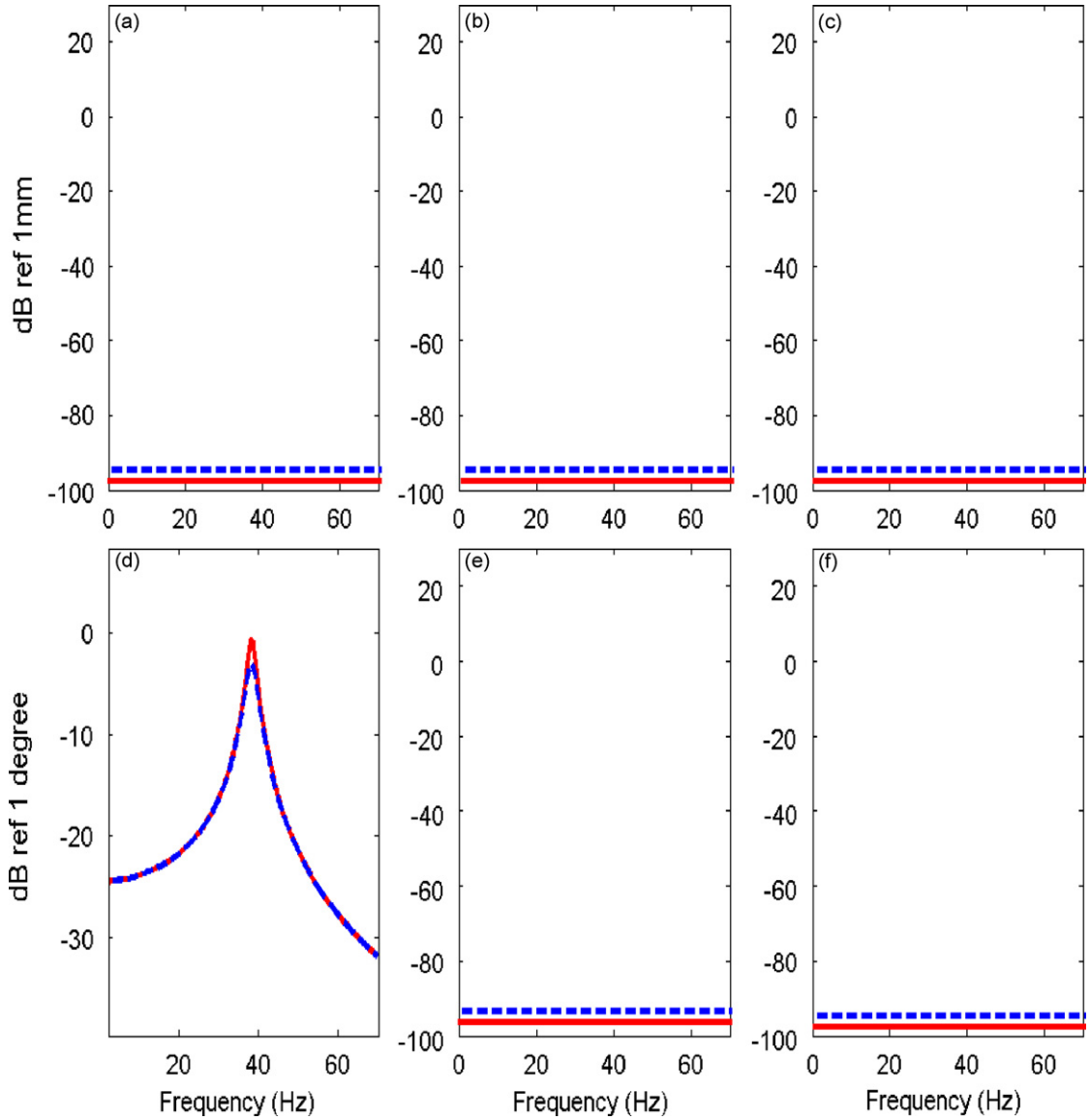

Fig. 8. Frequency-response functions given harmonic torque with torque roll axis decoupling scheme for non-proportional damping applied: (a) $X(\omega)$; (b) $Y(\omega)$; (c) $Z(\omega)$; (d) $\theta_X(\omega)$; (e) $\theta_Y(\omega)$; and (f) $\theta_Z(\omega)$. Key: — —, mounting system with proportional damping; ——, mounting system with non-proportional damping.

Table 4
Mount locations for torque roll axis decoupled mounting system for the focalized example

Mount #	1	2	3	4
Location (mm)				
r_x				
$\mathbf{C}_p$	318	318	−318	−318
$\mathbf{C}_N$	318	318	−318	−318
r_y				
$\mathbf{C}_p$	−198	198	−198	198
$\mathbf{C}_N$	−101	101	−198	198
r_z				
$\mathbf{C}_p$	−94	−94	−94	−94
$\mathbf{C}_N$	−150	−150	−94	−94

$\lambda_c(=-2\tau)$, are positive and real since **M**, **K**, and **C** are positive definite. Three eigenvalues (λ, λ_k, and λ_c) for the non-proportional damping case corresponding to the eigenvector, $\mathbf{q}_{\mathrm{TRA}}$, from three eigenvalue problems are related. The eigenvalue, $\lambda(=\tau+\mathrm{j}\eta)$, of the damped system is written in terms of λ_k and λ_c as $\lambda=-(\frac{1}{2})\lambda_c\pm\mathrm{j}\sqrt{\lambda_k-(\frac{1}{2}\lambda_c)^2}$. Like the proportional damping case, mounting system parameters such as the orientation angles (θ_i, φ_i, ϕ_i), stiffness and damping rate ratios ($L_{ki}=k_{ai}/k_{bi}$ and $L_{ci}=c_{ai}/c_{bi}$) and their locations ($\mathbf{r}_{mi}=[r_{xi}\ r_{yi}\ r_{zi}]^{\mathrm{T}}$) could be adjusted for the purpose to solve the above equations. Up to ten unknowns among the mounting parameters including the eigenvalues must be solved for since the rank of each matrix, $\mathbf{K}-\lambda_k\mathbf{M}$ or $\mathbf{C}_N-\lambda_c\mathbf{M}$, is at most five for a 6-dof mounting system due to its singularity property.

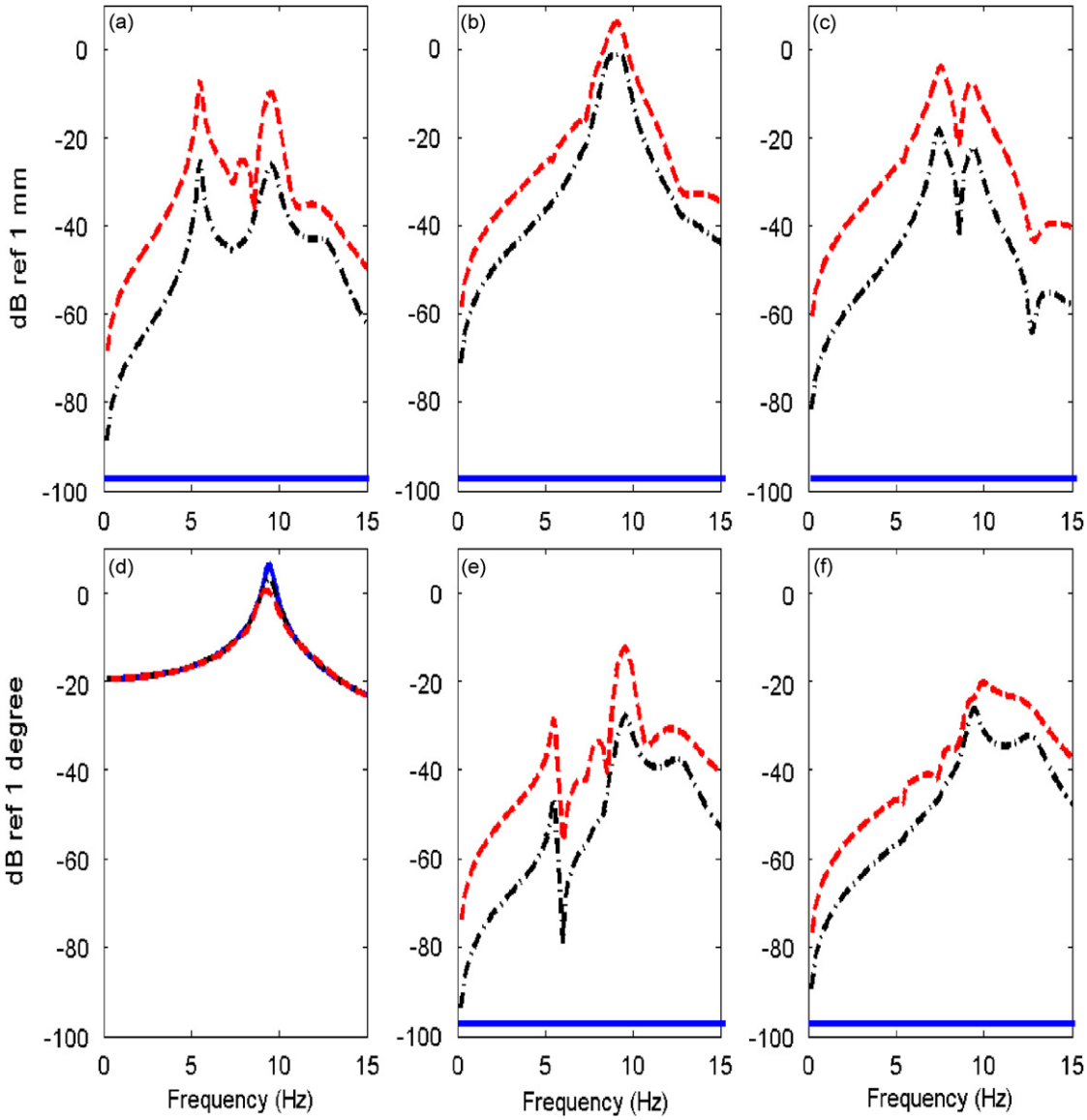

Fig. 9. Frequency-response functions for three values of non-proportional damping index (σ) given harmonic torque excitation with torque roll axis decoupling scheme for proportional damping applied: (a) $X(\omega)$; (b) $Y(\omega)$; (c) $Z(\omega)$; (d) $\theta_X(\omega)$; (e) $\theta_Y(\omega)$; and (f) $\theta_Z(\omega)$. Key: ——, $\sigma=0$; —·—, $\sigma=0.24$; — —, $\sigma=1.0$.

3.4. Non-proportional TRA decoupling for a focalized mounting system

In the focalized mounting system as shown in Fig. 6, an inertial coordinate system is chosen to be the same as the principal coordinate system and elastic centre lies on one of the principal axes, say the x-axis. Oscillating torque is assumed to be in the θ_X direction. It is the most desired case for the mounting system in terms of elastic axis focalization or TRA decoupling design since it would yield a complete decoupling given the torque excitation. A focalized mounting system with non-proportional damping is analyzed next and its mounting system parameters are as follows: mass $m = 50.5\,\mathrm{kg}$; moment of inertia ($\mathrm{kg\,m^2}$) $I_{XX} = 1.65$, $I_{YY} = 2.43$, $I_{ZZ} = 2.54$; inertia product ($\mathrm{kg\,m^2}$) $I_{XY} = I_{XZ} = I_{YZ} = 0$; stiffness $k_a = 8.4 \times 10^5\,\mathrm{N\,m^{-1}}$; stiffness rate ratio $L_k(= k_a/k_b) = 2.5$; mount orientation $\phi = 30^\circ$. Two highly damped mounts are used on one side (#1 and #2) with two poorly damped mounts on the other side (#3 and #4). The damping coefficients are as follows: low damping $c_{a\_L} = 300\,\mathrm{N\,s\,m^{-1}}$; low damping rate ratio $L_{c\_L}(= c_{a\_L}/c_{b\_L}) = 2.5$; high damping $c_{a\_H} = 3000\,\mathrm{N\,s\,m^{-1}}$; high damping rate ratio $L_{c\_H}(= c_{a\_H}/c_{b\_H}) = 25$. Overall response to the harmonic torque is shown in Fig. 7. The result is also compared with the response of a proportionally damped system when the TRA decoupling scheme (with proportional damping) is applied; in this case, four mounts with low damping are applied at four different positions. Even though the high damped mounts provide significant amplitude reduction in θ_X direction, coupled motions in y and θ_Z direction appear. The TRA decoupling for a non-proportionally damped mounting system is accomplished by assuming that the mounting parameters could be separately manipulated for stiffness and damping properties, respectively. The corresponding result is shown in Fig. 8 where it is also compared with the response of a proportionally damped system (when the TRA decoupling scheme with proportional damping is applied). Corresponding mount parameters for each eigenvalue problem are shown in Table 4. Note that $\mathbf{K}$ is designed for the proportional damping case based on $\mathbf{K}\mathbf{q}_{\mathrm{TRA}} = \lambda_k \mathbf{M}\mathbf{q}_{\mathrm{TRA}}$ for the TRA decoupling. Conversely, both $\mathbf{K}$ and $\mathbf{C}_N$ are constructed for the non-proportional damping case based on $\mathbf{K}\mathbf{q}_{\mathrm{TRA}} = \lambda_k \mathbf{M}\mathbf{q}_{\mathrm{TRA}}$ and $\mathbf{C}_N\mathbf{q}_{\mathrm{TRA}} = \lambda_c \mathbf{M}\mathbf{q}_{\mathrm{TRA}}$.

4. Conclusion

For non-proportionally damped mounting systems, analytical proofs are provided that show the TRA mode decoupling is possible when excited by the oscillating torque. While one eigenvalue problem, $\mathbf{K}\mathbf{q}_{\mathrm{TRA}} = \lambda_k \mathbf{M}\mathbf{q}_{\mathrm{TRA}}$, is required for proportional damping, two eigenvalue problems, $\mathbf{K}\mathbf{q}_{\mathrm{TRA}} = \lambda_k \mathbf{M}\mathbf{q}_{\mathrm{TRA}}$ and

Table 5
Mount parameters for the torque roll axis decoupled mounting system of a V6 engine with proportional ($\mathbf{C}_p$) and non-proportional ($\mathbf{C}_N$) damping cases

Mount parameters	Mount #			
	1	2	3	4
Stiffness				
k_a ($\mathrm{N\,mm^{-1}}$)	250	250	250	250
L_k	2.5	2.5	2.5	2.5
Location (mm)				
r_x				
$\mathbf{C}_p$	250	250	−250	−250
$\mathbf{C}_N$	250	250	−250	−250
r_y				
$\mathbf{C}_p$	−348	324	−286	340
$\mathbf{C}_N$	−181	180	−200	215
r_z				
$\mathbf{C}_p$	−55	−141	−143	−118
$\mathbf{C}_N$	−117	−119	−91	−70
Orientation (deg)				
ϕ	55	55	55	55

$\mathbf{C}_N\mathbf{q}_{\mathrm{TRA}} = \lambda_c\mathbf{M}\mathbf{q}_{\mathrm{TRA}}$, must be concurrently satisfied for the non-proportional damping case. Note that the TRA mode should be the corresponding eigenvector in either case.

Finally, we quantify the extent of non-proportionality by using the following index, σ, based on Nair and Singh's work [10]:

$$\sigma = \sum_{i=1}^{N}\sum_{j=1}^{N}|\mathbf{E}_{ij}| \quad \text{where } \mathbf{E} = \mathbf{C}\mathbf{M}^{-1}\mathbf{K} - \mathbf{K}\mathbf{M}^{-1}\mathbf{C}. \tag{31}$$

This examines deviations from the general condition for proportional damping: $\mathbf{C}\mathbf{M}^{-1}\mathbf{K} = \mathbf{K}\mathbf{M}^{-1}\mathbf{C}$ that was proposed by Caughey and O'Kelly [11]. The σ index is intentionally varied from a proportionally damped to highly non-proportionally damped system. Comparative spectra for the V6 diesel engine are shown in Fig. 9

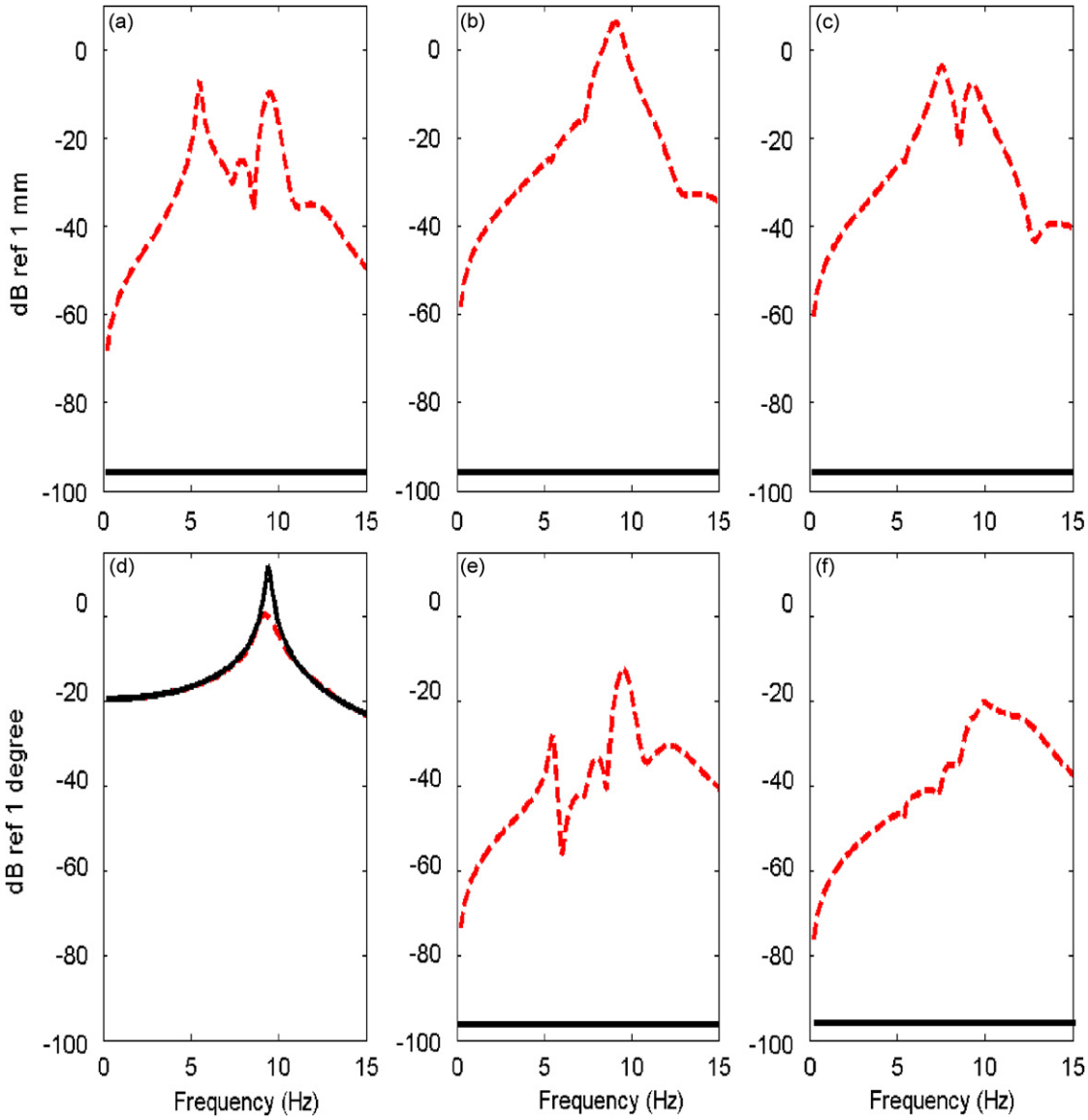

Fig. 10. Frequency-response functions given harmonic torque excitation for mounting system with non-proportional damping quantified by index ($\sigma = 1.0$ and 1.1): (a) $X(\omega)$; (b) $Y(\omega)$; (c) $Z(\omega)$; (d) $\theta_X(\omega)$; (e) $\theta_Y(\omega)$; and (f) $\theta_Z(\omega)$. Key: — —, torque roll axis decoupling scheme (with proportional damping) is applied ($\sigma = 1.0$); ——, torque roll axis decoupling scheme (with non-proportional damping) is applied ($\sigma = 1.1$).

where the damping in one of the mounts is changed by 1, 3, and 10 times the nominal (proportional) damping values, respectively. The σ index is normalized with respect to the maximum value to be 0, 0.24, and 1. The two eigenvalue problems developed for non-proportionally damped case are also applied to the V6 engine mounting system. The non-proportional damping is formulated by using highly damped mounts at two positions with $\sigma = 1.10$. For the roll mode decoupling given torque excitation, mount locations are sought in order to construct $\mathbf{K}$ and $\mathbf{C}_N$ based on two eigenvalue problems that were previously developed; these are listed in Table 5. The frequency responses are indeed decoupled as shown in Fig. 10; for the sake of comparison, coupled responses (as calculated previously without using the proposed design concept) are also depicted. It is seen that magnitude in the rolling motion increases when the TRA decoupling scheme (with non-proportional damping) is applied. Essentially, it is due to a reduction in damping in the roll direction. From the results shown in Fig. 9, a higher value of σ would induce more coupling between the motions. But, Fig. 10 indicates that the TRA decoupling is indeed achieved even for a mounting system with high non-proportional damping as long as the proposed design concept is employed.

Our examples show that the proposed axioms work properly even though there is practical limitation on the premise that both damping and stiffness elements could be separately manipulated to achieve the desired decoupling. Further complications arise from spectrally varying and amplitude-sensitive stiffness and damping properties of the engine mounts, as well as from the compliance of flexible base. Further work along those lines is in progress.

References

[1] T. Jeong, R. Singh, Analytical methods of decoupling the automotive engine torque roll axis, *Journal of Sound and Vibration* 234 (2000) 85–114.
[2] C.M. Harris, *Shock and Vibration Handbook*, McGraw-Hill, New York, 1995 (Chapter 3).
[3] J. Bang, H. Yoon, K. Won, Experiment and simulation to improve key on/off vehicle vibration quality, Society of Automotive Engineering Paper 2007-01-2363, 2007.
[4] Y. Yu, N.G. Naganathan, R.V. Dukkipati, Review of automotive vehicle engine mounting systems, *International Journal of Vehicle Design* 24 (4) (2000) 299–319.
[5] E.E. Ungar, C.W. Dietrich, High-frequency vibration isolation, *Journal of Sound and Vibration* 4 (2) (1966) 224–241.
[6] H. Ashrafiuon, Design optimization of aircraft engine mount systems, *Journal of Vibration and Acoustics—Transactions of the ASME* 115 (4) (1993) 463–467.
[7] H. Ashrafiuon, C. Nataraj, Dynamic analysis of engine-mount systems, *Journal of Vibration and Acoustics—Transactions of the ASME* 14 (1) (1992) 79–83.
[8] C.E. Spiekermann, C.J. Radcliffe, E.D. Goodman, Optimal design and simulation of vibrational isolation systems, *Journal of Mechanisms Transmissions and Automation in Design* 107 (1985) 271–276.
[9] J.S. Tao, G.R. Liu, K.Y. Lam, Design optimization of marine engine-mount system, *Journal of Sound and Vibration* 235 (2000) 477–494.
[10] S.S. Nair, R. Singh, Examination of the validity of proportional damping approximations using two numerical indices, *Journal of Sound and Vibration* 104 (1986) 348–350.
[11] T.K. Caughey, M.E.J. O'Kelly, Classical normal modes in damped linear dynamic systems, *Journal of Applied Mechanics* 32 (1965) 583–588.